Abdominal Imaging

Published online: 30 January 2006

Abdom Imaging (2006) 31:461–482
DOI: 10.1007/s00261-005-0394-5

UPDATE

Imaging of the renal transplant: comparison of MRI with duplex sonography

R. F. J. Browne, D. J. Tuite

Department of Radiology, The Adelaide and Meath Hospital, Tallaght, Dublin 24, Ireland

Abstract

Renal transplantation is an established treatment for patients with end-stage renal disease. Many causes of graft dysfunction are treatable, making prompt detection and diagnosis of complications essential. Sensitive, noninvasive imaging procedures, which do not use iodinated contrast media, are therefore highly desirable to evaluate graft function. Duplex sonography (US) has traditionally been the initial investigation of graft dysfunction. US offers many advantages, particularly during the postoperative period, when it can be performed portably regardless of renal function and can guide percutaneous procedures. However, US lacks specificity in assessing hydronephrosis, cannot differentiate parenchymal causes of dysfunction, and may have difficulty assessing transplant vessels. Recently comprehensive magnetic resonance imaging (MRI) protocols including MR urography, gadolinium-enhanced MR angiography, and MR renography have evolved as a ''one-stop'' diagnostic technique in the evaluation of the entire graft and peritransplant region. Multiplanar capabilities enable MRI to identify the site of urinary obstruction and assess renal vessels in their entirety. The evolving technique of MR renography may also differentiate parenchymal causes of dysfunction. By combining these three components into a single examination, further information may be obtained regarding the graft when compared with US and other conventional studies, with improved patient convenience, less morbidity, and a potential cost saving.

Key words: Ultrasound—Magnetic resonance imaging—Renal transplant

Renal transplantation is a successful and cost-effective treatment for patients with end-stage renal disease [1]. For many patients with chronic renal failure, a well-functioning graft can mean a return to a normal and independent lifestyle. The limited number of donor kidneys, however, makes ensuring graft survival paramount.

Currently the average normal life expectancy of a transplanted cadaveric kidney is 7 to 10 years, which increases to 15 to 20 years when a live donor organ is used [1]. This has been aided by improved surgical techniques, effective immunosuppressive regimens, improved histocompatibility matching, and close graft surveillance. Many causes of renal graft dysfunction are treatable, making prompt detection and diagnosis of complications essential. Sensitive, noninvasive imaging procedures to evaluate the renal transplant are therefore highly desirable and can improve graft survival rates. Duplex sonography (US) has traditionally been the initial investigation performed in the assessment of graft dysfunction [2, 3]. US is inexpensive, uses no ionizing radiation, and is readily acceptable to clinicians and patients. The superficial location of the graft within the iliac fossa makes it ideal for US assessment. In the postoperative period, US can be repeated at the bedside regardless of graft function to detect correctable causes of graft dysfunction, and it can facilitate percutaneous biopsy or drainage. US has also proved to be an effective screening modality for detecting graft vascular complications [4]. However, US lacks specificity in determining the cause of hydronephrosis, provides no functional assessment, and cannot differentiate parenchymal causes of dysfunction [3]. US may also have difficulty assessing transplant vessels due to anatomical and technical limitations. Further disadvantages inherent to all US examinations are the influence of different machines, different operators, and interobserver variability.

Recently magnetic resonance imaging (MRI) has emerged as an alternative imaging modality in renal transplant graft assessment. MRI is promising due to its multiplanar capabilities and lack of ionizing radiation,

Correspondence to: R. F. J. Browne; *email:* ronan.browne@amnch.ie

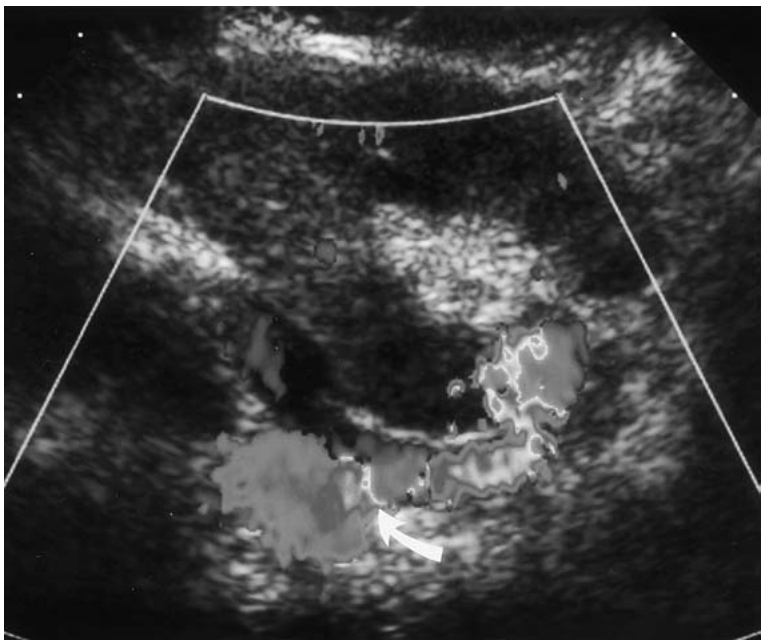

Fig. 1. Transverse color Doppler US shows normal end-to-side anastomosis of the renal artery to the external iliac artery (*arrow*).

invasiveness, and contrast medium-induced nephrotoxicity. Recent studies have shown the utility of MRI in the evaluation of the renal graft and peritransplant region, but its role is not yet firmly established [5].

Gadolinium-enhanced magnetic resonance angiography (MRA) is well established in native renal artery assessment, comparing well with conventional angiography (DSA), and is becoming established as an accurate, safe, and rapid technique in the assessment of the transplant vasculature [6–10]. Improved temporal resolution and repeated sequences after contrast administration allow optimal and separate enhancement of the arteries and veins. Recently various MRI sequences have been combined to give information regarding anatomy, function, vascular flow and lesion characterization in the transplant kidney [5]. An MRI protocol using magnetic resonance urography (MRU), gadolinium-enhanced MRA, and gadolinium-enhanced T1-weighted coronal parenchymal imaging (MR renography) offers a one-stop diagnostic technique in the evaluation of the entire renal transplant and peritransplant region. Similar "one-stop shop" MR protocols have been used to preoperatively evaluate potential living kidney donors, with findings comparable with those of other modalities [11, 12].

This report discusses the current role of US and MRI in graft assesment in the immediate postoperative period and in routine follow-up. For the purpose of this discussion, renal graft dysfunction has been categorized into extrinsic, vascular, and parenchymal causes. Extrinsic causes include peritransplant fluid collections such as urinoma, lymphocele, abscess, and hematoma or ureteral obstruction. Vascular causes include stenosis, thrombosis, or occlusion of the transplant or native iliac vessels. Parenchymal causes include acute tubular necrosis (ATN), rejection, and medication toxicity. The relative merits and limitations of both modalities in the assessment of these graft complications are addressed.

Anatomy

The renal transplant graft is usually placed extraperitoneally within the right iliac fossa. In general, the transplant vessels are anastomozed to the external iliac artery and vein in the case of a cadaveric transplant and to the internal iliac vessels in a live related transplant. The renal artery is typically anastomosed end to side with the external iliac artery (Figs. 1, 2) or end to end with the internal iliac artery. The renal vein to external iliac vein is typically end to side. The ureterovesical (UV) anastomosis is fashioned by attaching the shortened donor ureter to the dome of the bladder. As a consequence of this procedure, the lower end of the ureter, particularly if left too long, is prone to ischemic insult and subsequent stricture formation, which can be functionally significant.

US imaging technique

Usually a 3.5- to 4-MHz probe provides good overall assessment of the transplant graft and perigraft region. A higher frequency probe can be used to improve near field resolution and anatomic detail, if required. The graft is often best visualized from an anterolateral approach with displacement of any overlying bowel loops with gentle compression. Renal morphologic characteristics and size are first evaluated with gray-scale US in the longitudinal and transverse planes. Volume measurements are calculated and compared with previous measurements, if available. The collecting system and

Fig. 2. Anteroposterior oblique MIP shows normal end-to-side anastomosis of the renal artery to the external iliac artery (*arrow*).

perigraft region are then assessed for dilatation or extrinsic fluid collections. An initial scan with power or color Doppler to demonstrate areas of decreased flow can be useful. Color and spectral Doppler analysis of the ipsilateral iliac artery proximal and distal to the anastomosis, the renal artery, and the interlobar vessels of the upper, middle, and lower poles of the kidney is then performed. The following spectral parameters are routinely evaluated: peak systolic velocity (PSV), acceleration time (AT), and resistive index (RI). The ratio of the PSV in the renal and external iliac arteries is also calculated. It is important that the Doppler angle be kept at 30 to 60° for vascular assessment. At our institution an RI lower than 0.75 to 0.8 is taken as normal. The normal renal arterial waveform reflects a low-resistance system, with diastolic flow contributing up to a third or even half of the PSV (Fig. 3). The main renal vein usually displays a normal antegrade venous waveform. US is usually performed in the first 24 to 48 h after surgery to establish a baseline and subsequently based on clinical/biochemical parameters.

MRI technique

At our institution MRI examinations are performed on a 1.5-T commercially available scanner using a phased-array body coil. Fifteen milliliters of gadobutrol is administered intravenously for the contrast portion of the study.

All patients undergo the following sequences with parameters as shown:

1. Multiplanar half Fourier acquisition single-shot turbo spin echo (HASTE) MRU (TR/TE/flip angle 1110 ms/119 ms/123°), scan matrix 512, one excitation, field of view 350 mm, and 29- × 3-mm interpolated slices (Fig. 4).
2. Gadolinium-enhanced MRA and MRV using a fast-spoiled gradient echo technique (TR/TE/flip angle 3.64 ms/1.34 ms/25°), scan matrix 512, one excitation, field of view 440 mm, and 64- × 1.5-mm interpolated slices. A timing bolus is used to determine the time to peak arterial enhancement and estimate injection to scan delay. Three-dimensional (3D) images are obtained during breath holding in the arterial and venous phases of contrast enhancement. Reconstruction is performed by using operator-defined maximum intensity projections (MIPs; Fig. 2).
3. Gadolinium-enhanced T1-weighted coronal MRI (MR renography). Repeat datasets are obtained during arterial, venous, and equilibrium phases with separate breath holds. The rate of contrast material transit in the kidney is assessed and changes in renal enhancement are evaluated (Fig. 5).

Obstruction/peritransplant fluid collections

Urinary obstruction and leaks are potentially life-threatening renal graft complications. In the immediate postoperative period, edema at the ureteric anastomosis often results in mild transient hydronephrosis. If renal

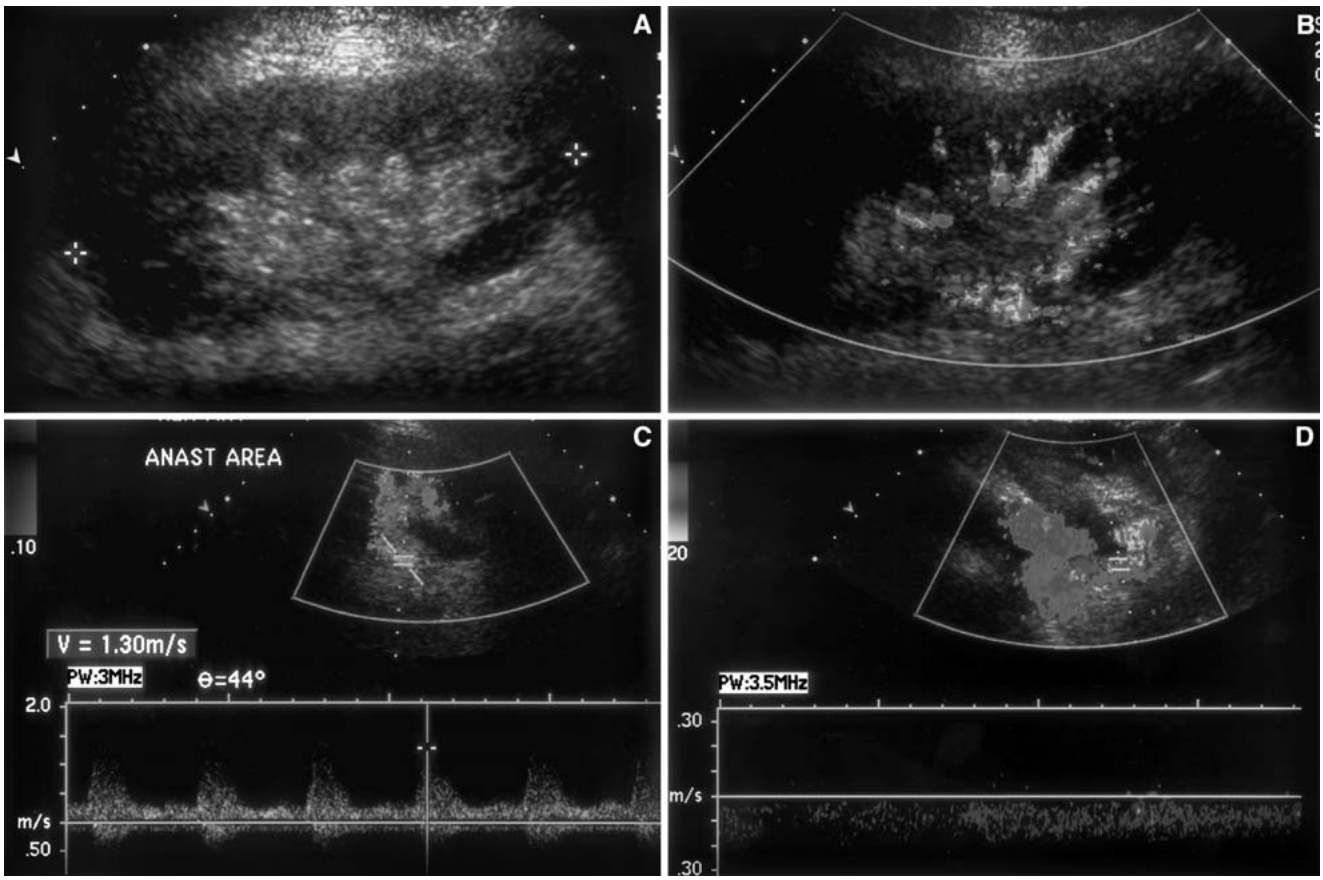

Fig. 3. Normal graft appearances on US. **A** Longitudinal gray-scale US. **B** Color Doppler US. **C** Spectral tracing renal artery. **D** Spectral tracing renal vein.

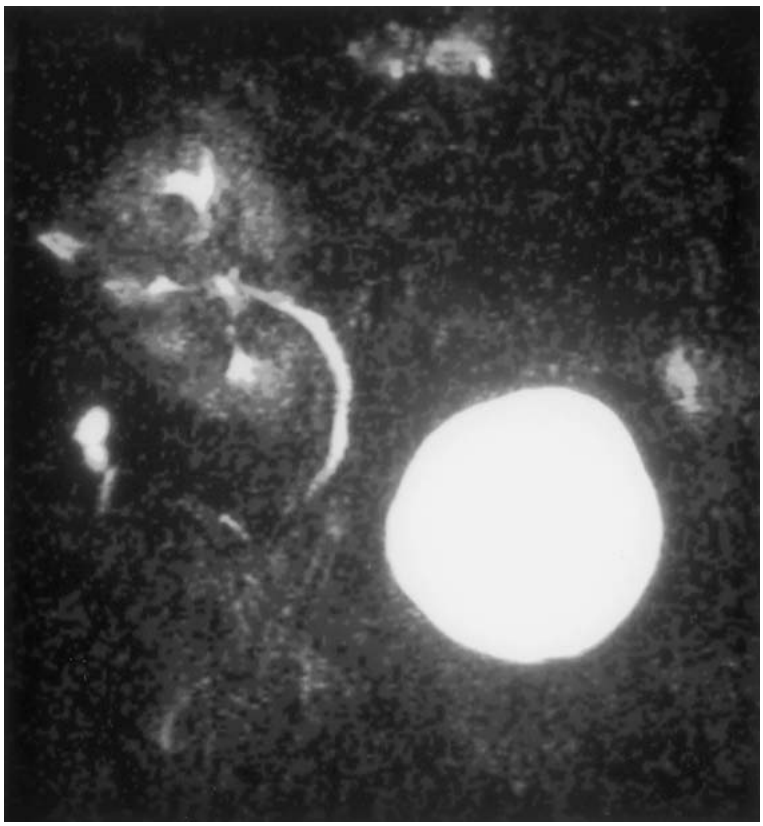

Fig. 4. Coronal HASTE MRU source image shows normal graft collecting system appearances.

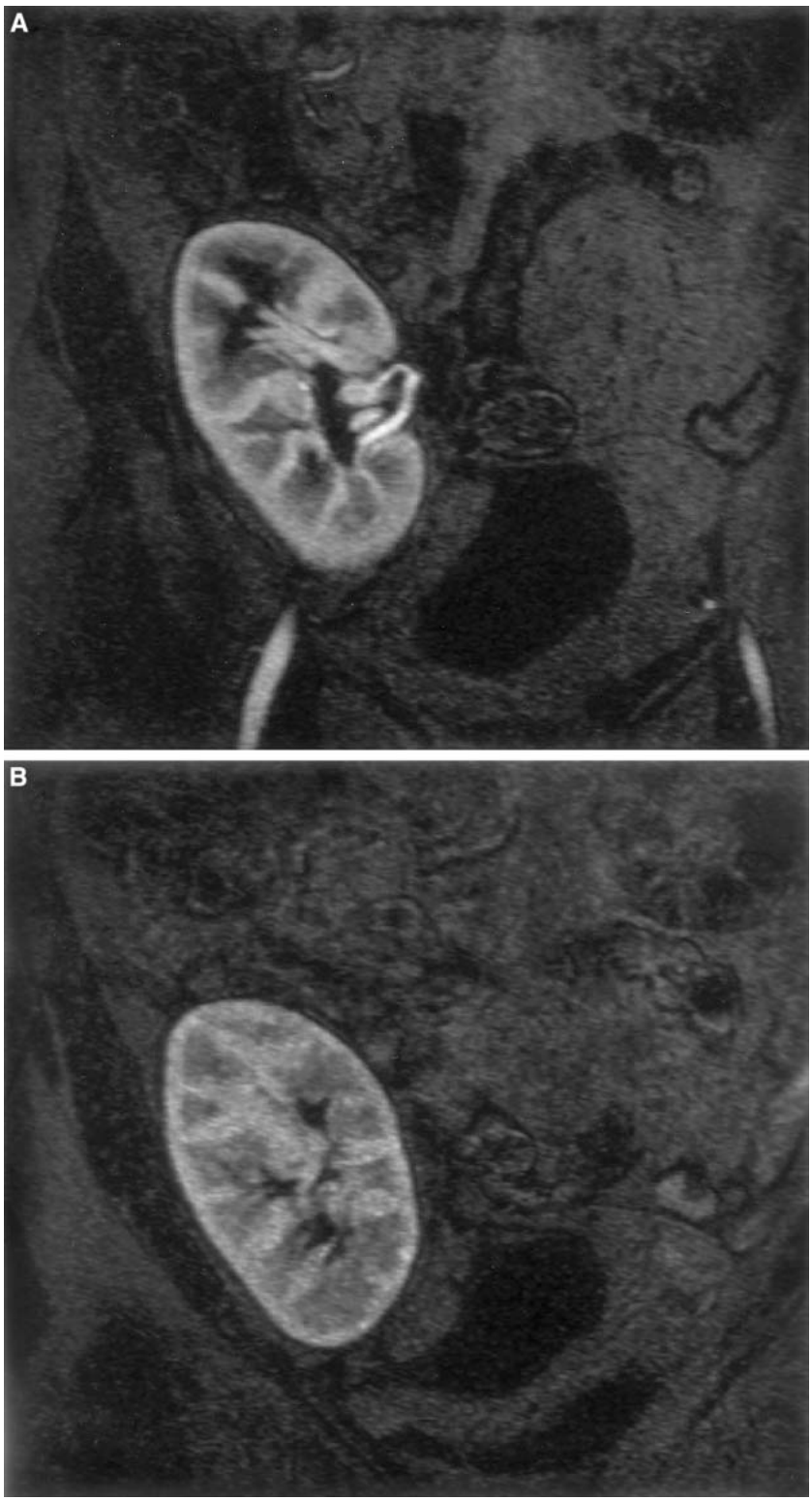

Fig. 5. Coronal MR renography shows normal graft appearances in (**A**) arterial and (**B**) mixed venous phases of enhancement.

function is abnormal, this must be differentiated from true obstruction, which occurs in up to 10% within 3 months of surgery [13]. Ureteric ischemia and stenosis account for approximately 90% of obstruction and invariably involves the distal ureter close to the UV junction [13]. Obstruction may also occur secondary to rejection or ureteric compression from a perigraft collection. Rarely obstruction from clot, calculi, fungus balls, or sloughed papillae may occur. Perigraft collections occur in about 14% in the early postoperative

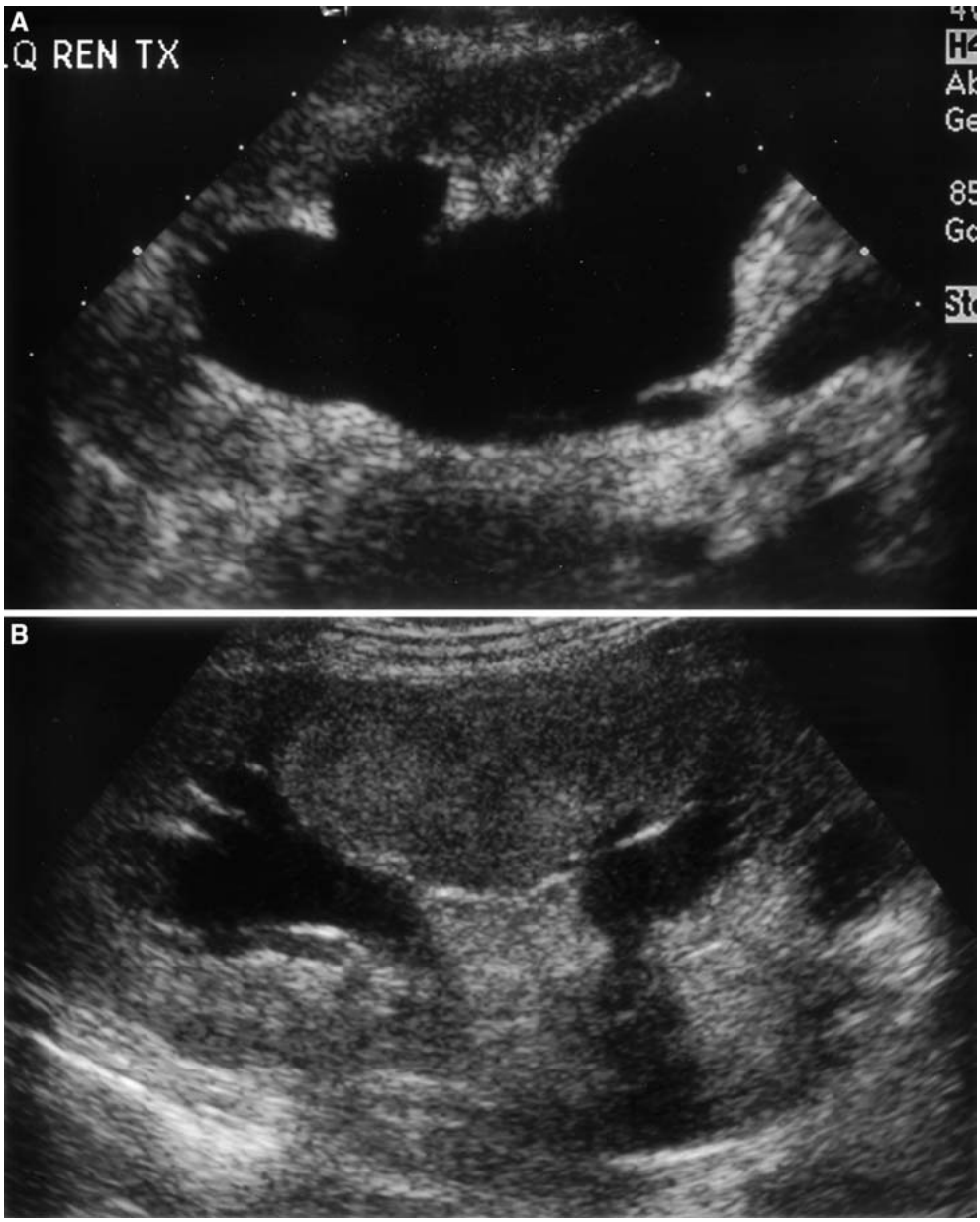

Fig. 6. Graft collecting system obstruction. **A** Longitudinal gray-scale US shows severe graft hydronephrosis secondary to an obstructing urinoma diagnosed on US. **B** Longitudinal gray-scale US shows graft hydronephrosis secondary to a ureteric stricture, diagnosed on antegrade pyelography.

course [13]. These may be incidental and effects on renal function depend on their size and location. Urinary leaks occur in 1% to 5%, usually from UV anastomotic breakdown or the distal ureter secondary to mucosal ischemia and necrosis [13]. These typically occur in the first 2 weeks and cause perigraft urinomas, which must be differentiated from hematomas and lymphoceles, which may not require treatment. Differentiation can be attempted based on time interval after transplantation: lymphoceles typically occur 4 to 8 weeks after surgery, whereas urinomas and hematomas develop in the very early postoperative period [4].

Lymphoceles are attributed to disruption of recipient lymphatics at the time of graft placement and typically develop medially or inferior to the lower pole of the kidney. US is sensitive and specific for hydronephrosis [14] (Fig. 6). US in general, however, provides limited views of the ureter and UV anastomosis and therefore often does not identify the cause or site for obstruction or the site of urinary leak [15, 16].

Antegrade pyelography, which is usually performed under US guidance, is therefore often required to determine the functional significance of hydronephrosis, demonstrate true obstruction, or identify the site of urinary leak. In the case of a known obstruction, US can guide percutaneous nephrostomy to divert urinary flow and assess the relative contribution of obstruction to overall transplant dysfunction.

Further treatment such as ureteric stenting or balloon dilatation can then be undertaken, although surgical

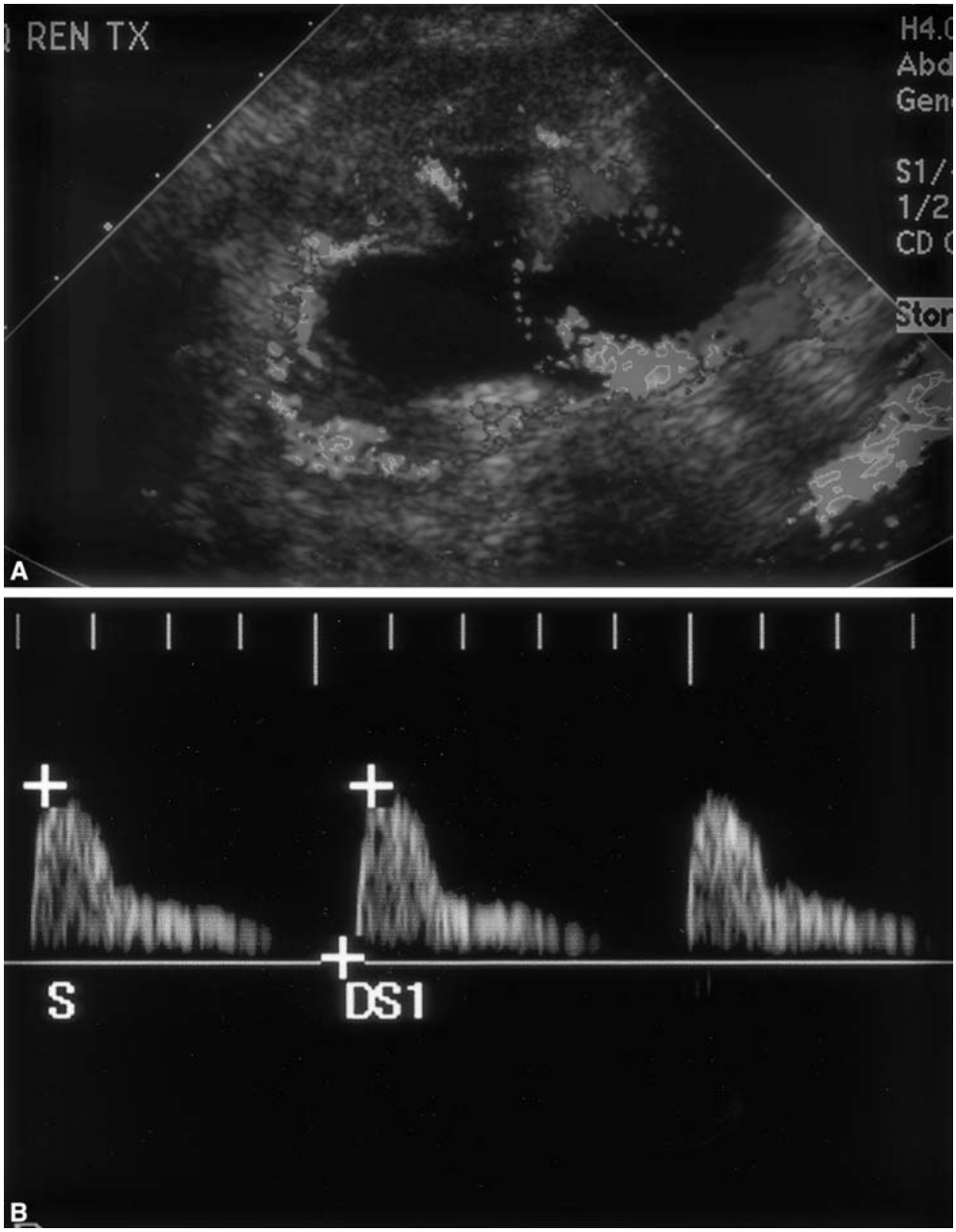

Fig. 7. Graft hydronephrosis with elevated RI. **A** Longitudinal color Doppler US shows graft hydronephrosis. **A** Spectral tracing from an intrarenal artery shows elevated RI secondary to hydronephrosis.

revision may ultimately be required [13]. Obstructive pyelocaliectasis is usually associated with an elevated RI on Doppler analysis, although this is too nonspecific to be a reliable diagnostic parameter [4] (Fig. 7). Echoes within the collecting system may suggest pyo- or hemonephrosis. The US characteristics of perigraft fluid collections are nonspecific and US-guided percutaneous aspiration is often required to differentiate [17] (Fig. 8). Urinomas are high in creatinine, whereas lymphoceles are rich in protein and cholesterol with normal creatinine. Septations may be seen in all collections, especially if infection coexists (Fig. 9). Lymphoceles only require treatment if symptomatic, infected, or if causing obstruction, where drainage should be combined with instillation of a sclerosing agent [13]. Urinomas and infected collections should be percutaneously drained, usually under US guidance, and portably, if necessary.

MRU has great sensitivity for fluid detection and allows identification of hydronephrosis, peritransplant fluid collections, and intraparenchymal cysts [18, 19] (Figs. 10, 11). Static MRU uses fast, heavily T2-weighted sequences that display high-resolution images of the fluid-filled urinary tract, without the potential side effects of iodinated contrast medium administration. A fat-suppression pulse allows decreased signal intensity of retroperitoneal fat, further improving visualization of the urinary tract [18]. Acquisition times of approximately 1 s per slice allow uncooperative and ill patients to be im-

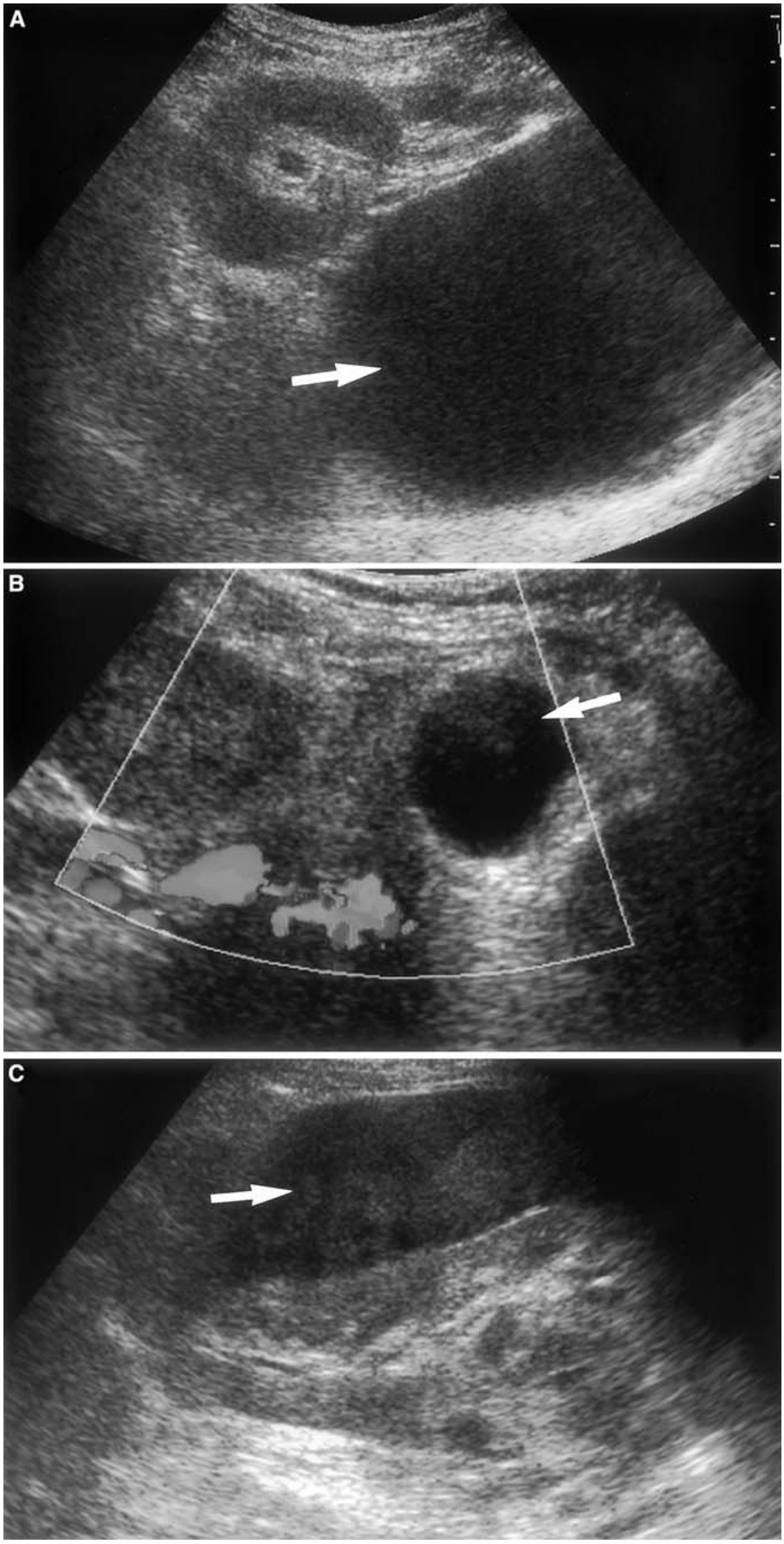

Fig. 8. Perigraft fluid collections. **A** Transverse gray-scale US shows a large urinoma (*arrow*). **B** Transverse color Doppler US demonstrates a small lymphocele (*arrow*). **C** Longitudinal gray-scale US displays a large mixed echogenic perinephric hematoma (*arrow*).

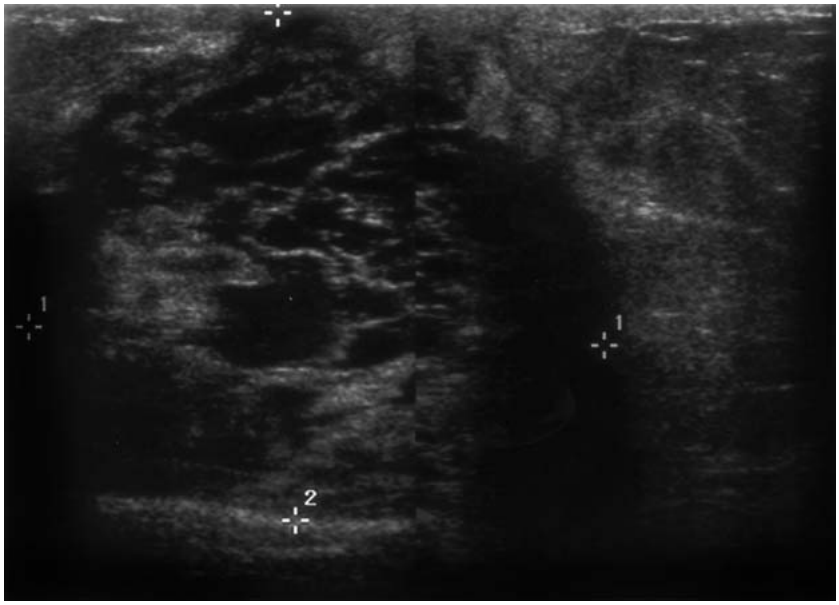

Fig. 9. Longitudinal gray-scale US depicts a superficial multiloculated mixed echogenic abscess collection.

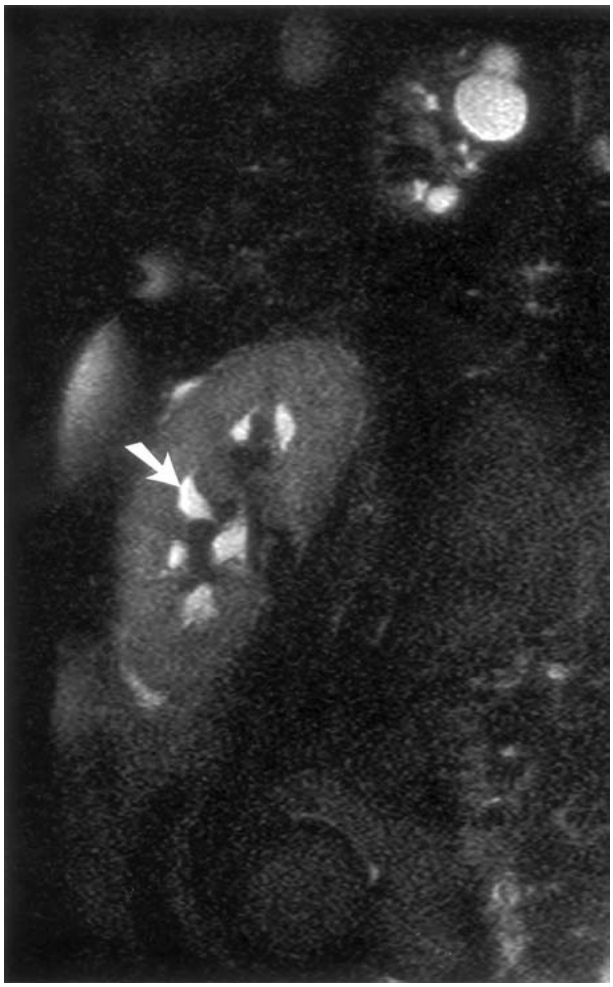

Fig. 10. Sagittal HASTE MRU source image shows mild graft hydronephrosis (*arrow*).

aged, which is especially relevant in failing transplants, where long acquisition times may not be tolerated. In obstruction the stasis of urine and dilatation of the collecting system provide a column of static fluid, allowing excellent evaluation and localization of the exact site of obstruction [3, 15, 18] (Fig. 12). MRU has been shown to be superior to excretory urography (EU) and US in demonstrating the urinary tract distal to the level of obstruction [20]. Although antegrade pyelography remains the gold standard in the differentiation of complete from incomplete obstruction, it is invasive with a significant complication rate [3]. MRU offers a potentially noninvasive way of differentiating true obstruction from transient hydronephrosis because the ureter can usually be visualized in its entirety.

Dynamic MRU after gadolinium, although not routinely performed as part of our protocol, can further help differentiate because graft excretion of contrast can be directly assessed on delayed images (Fig. 13). Dynamic MRU can also differentiate a urinoma from other perigraft collections because contrast will accumulate in the collection and identify the site of leak. Formerly antegrade pyelography or nuclear medicine renography were required to demonstrate this [13]. Lymphoceles, urinomas, abscesses, and hematomas are all high-signal intensity on MRU (Fig. 14). Hematomas, however, would be expected to have a high signal component on T1-weighted sequences, unlike urinomas or lymphoceles, which will be of lower signal intensity. Abscesses tend to have thickened walls that enhance after gadolinium administration.

Vascular assessment

Renal artery stenosis (RAS), occurring in up to 12% of post-transplantations, may be due to atherosclerotic

Fig. 11. Sagittal HASTE MRU source image demonstrated perinephric fluid (*arrow*).

disease or surgical trauma [2, 4, 5, 21]. This manifests as hypertension or loss of function in the absence of rejection, obstruction, or infection and accounts for more than 75% of all vascular complications [13]. Typically it occurs at the site of anastomosis that connects the transplant artery to the native iliac artery [6]. A stenosis of 70% or greater is deemed as hemodynamically significant [8]. The age of onset can be variable and, although the outcome of untreated RAS is not known, balloon angioplasty or arterial stenting is the accepted treatment [22, 23].

These procedures, however, carry a significant complication profile. An accurate imaging modality, which can assess the transplant vascular system noninvasively, is therefore highly desirable. Renal artery thrombosis (RAT) and renal vein thrombosis (RVT) occur less commonly, usually early in the postoperative period. Predisposing causes include poor surgical technique, compression by fluid collections, and hypovolemia [4]. Early diagnosis and treatment is essential to prevent premature loss of allograft. Arterial false aneurysms and arteriovenous (AV) fistulas occur in 1% to 2%, invariably after percutaneous biopsy, although most are small and resolve uneventfully. Large ones may require treatment with transcatheter embolization.

Doppler US has traditionally been used to assess the transplant vasculature and has proved to be an excellent, noninvasive screening modality [24]. The success of Doppler US detection of stenoses is highly dependent on direct visualization of the renal vessels and anastomoses, usually at the external iliac artery and vein. Gray-scale US morphologic findings in RAS include focal wall narrowing, thickening, and calcification. Color Doppler US assesses overall vessel patency. On color Doppler US stenotic segments appear as regions of focal color aliasing indicative of high velocity, which are further assessed

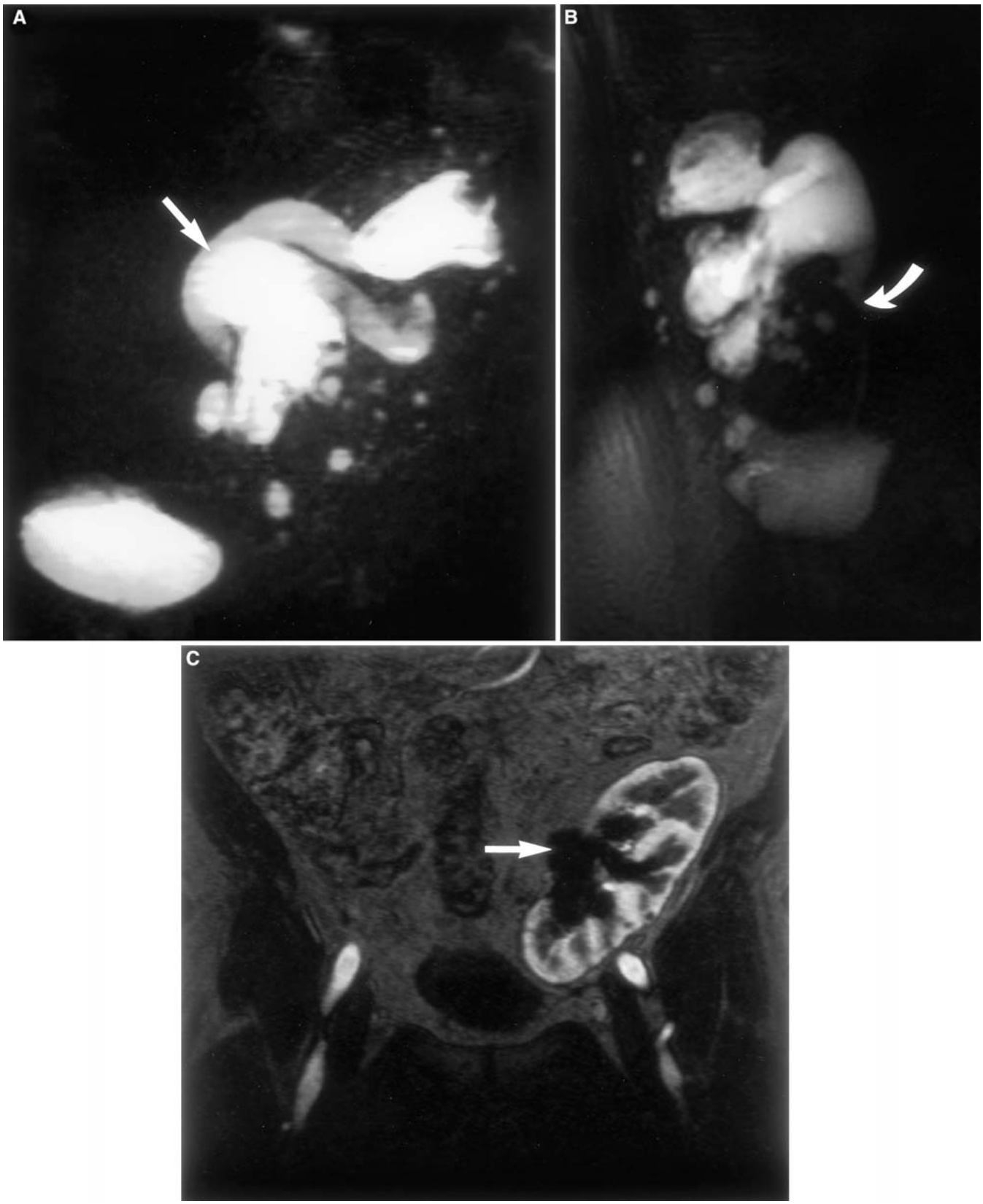

Fig. 12. Ureteric stenosis. **A** Sagittal HASTE MRU source image shows severe graft hydronephrosis (*arrow*). **B** Sagittal MIP MRU displays graft hydronephrosis that is secondary to a proximal ureteric stenosis (*arrow*). **C** Coronal MR renography also shows graft hydronephrosis (*arrow*).

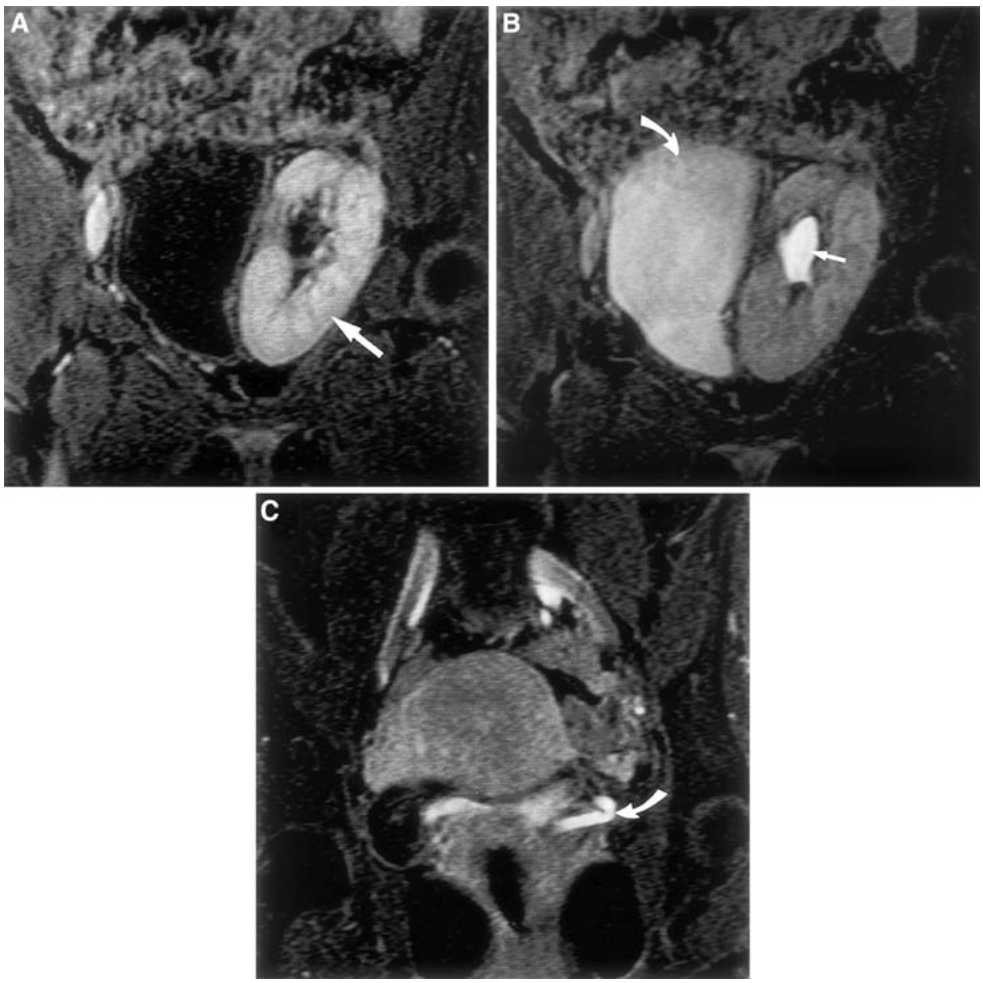

Fig. 13. Coronal dynamic MRU. **A** Imaging at 45 s after injection shows contrast in the renal parenchyma (*arrow*). **B** Delayed imaging at 4 min demonstrates contrast in the renal collecting system (*straight arrow*) and bladder (*curved arrow*). **C** Mild hydronephrosis is secondary to a kink in the ureter (*arrow*).

by spectral analysis. Spectral Doppler analysis allows absolute velocity and gradients to be determined, which are the most useful diagnostic parameters. An elevated PSV is considered to be the hallmark of a significant stenosis (Fig. 15). A PSV of 2 to 2.5 m/s has been advocated as suspicious for RAS [1, 4, 22, 24]. Other investigators have advocated a value higher than 3 m/s to improve specificity and decrease unnecessary arteriography, particularly when dealing with a low-risk or surveillance population [22]. An AT of 0.1 s or higher in the renal and intrarenal arteries, a ratio of PSVs in the renal and external iliac arteries greater than 1.8, and focal Doppler frequency shift (>7.5 KHz) are also highly accurate in diagnosing RAS [4, 25–27]. However, Doppler assessment of the artery can be technically challenging because the entire length of the vessel has to be clearly imaged and the angle-corrected ($<60°$) PSV recorded [25]. Spectral broadening and elevated PSV may be observed in normal vessels at anastomotic sites, curves, and kinks, leading to false-positive results and problems in reliably excluding the diagnosis [1, 27–29]. Because extrarenal arteries may be technically difficult to assess, downstream hemodynamic repercussions in the distal intrarenal arterial bed may need to be assessed to diagnose RAS [26, 30]. Tight stenoses may exhibit a downstream spectral broadening or prolonged early acceleration and diminished amplitude of arterial systole (tardus-parvus pattern; Fig. 16), which may be limited to a portion of the kidney if an RA branch is involved. Most studies on the tardus-parvus effect have been conducted on native kidneys and the clinical significance in transplanted kidneys is not fully established [26]. The most reliable diagnostic criteria are therefore those obtained from the stenotic site. In total RA occlusion a mute RA is visualized in conjunction with severe intrarenal velocity abnormalities.

Renal vein stenosis, although less common, causes color aliasing secondary to focal high velocity at the point of stenosis. RAT demonstrates absent intrarenal venous and arterial flow, although severe rejection or RVT can occasionally mimic these findings [4] (Fig. 17). Absent flow in the main renal artery will differentiate RAT from these other entities. In RVT the graft may appear swollen and hypoechoic but US diagnosis relies on the detection of echogenic thrombus within a mute or partially flowing renal vein. RVT is also associated with

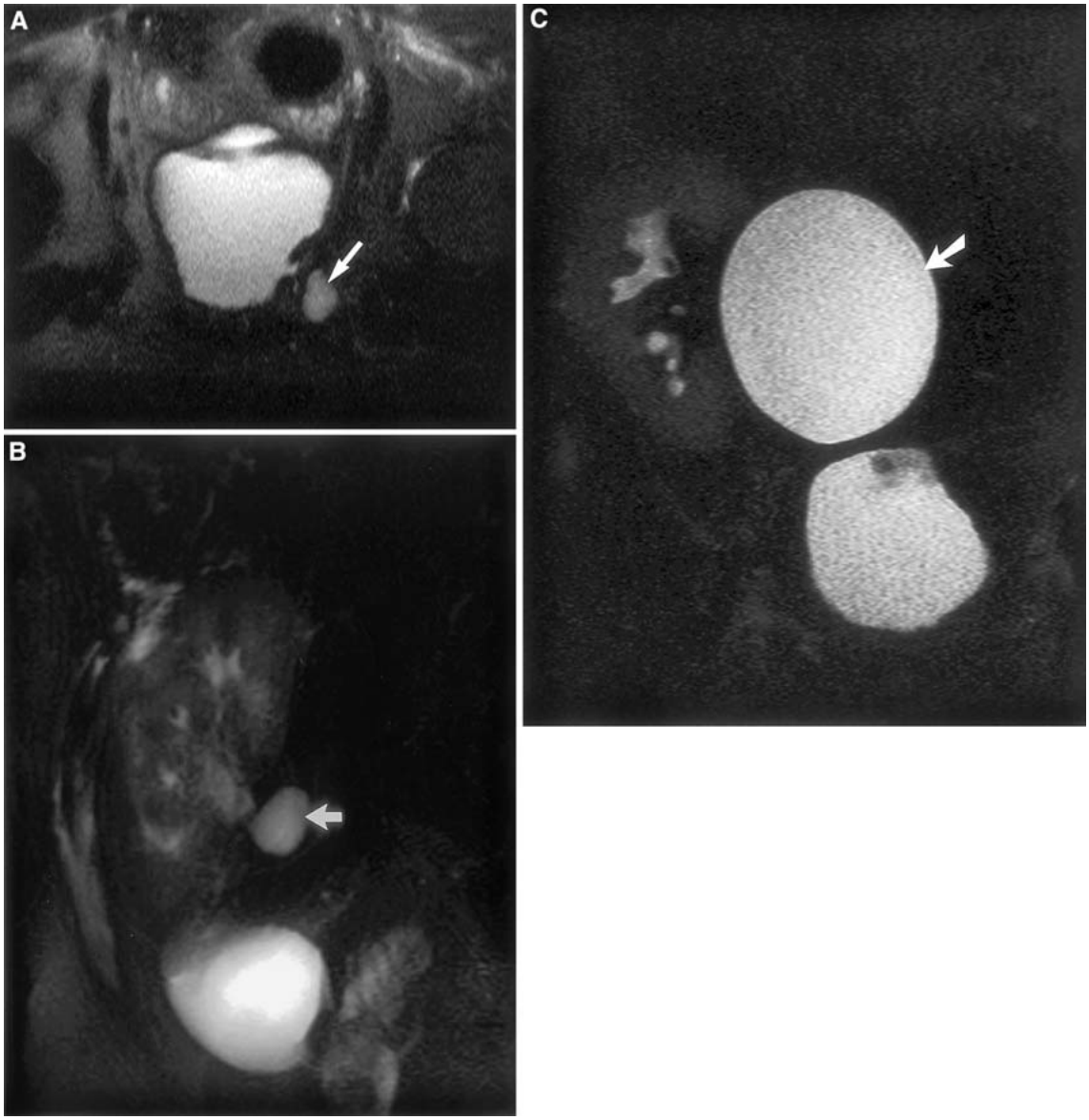

Fig. 14. Perigraft fluid collections. **A** Axial HASTE MRU source image shows a small lymphocele at the anterolateral aspect of the bladder (*arrow*). **B** Sagittal HASTE MRU source image demonstrates a small lymphocele posteroinferior to the renal graft (*arrow*). **C** Coronal HASTE MRU source image displays a large urinoma superior to the bladder, causing mild graft hydronephrosis (*arrow*).

absent intrarenal venous flow and high arterial RI with plateau-like retrograde diastolic flow because, unlike in native vessels, collateral venous supply does not develop [30]. Partial RVT may be manifest only as a nonspecific increase in arterial resistance. Reversed diastolic flow itself is nonspecific and may be caused by acute rejection or ATN [4, 14]. False aneurysms result from a site of arterial injury without venous drainage and are therefore seen as a hypoechoic round mass located within the renal parenchyma that fills with color on Doppler analysis. A typical to-and-fro sign is seen on spectral tracing at the level of the communicating channel. AV fistulae may appear as a focal flurry of disorganized color flow, containing arterial and venous components, outside the borders of the normal renal vasculature (Fig. 18). Highly turbulent flow at the site of the shunt can be differentiated from "high flow" in other areas by increasing the pulse repetition frequency to a level that results in non-visualization of the normal renal vasculature. Flow velocity is increased in the feeding artery with a marked decrease in RI values. The draining vein exhibits an increase flow velocity with systolic-diastolic modulation. The use of contrast-enhanced US has recently been shown to improve detection of renal vessels and diag-

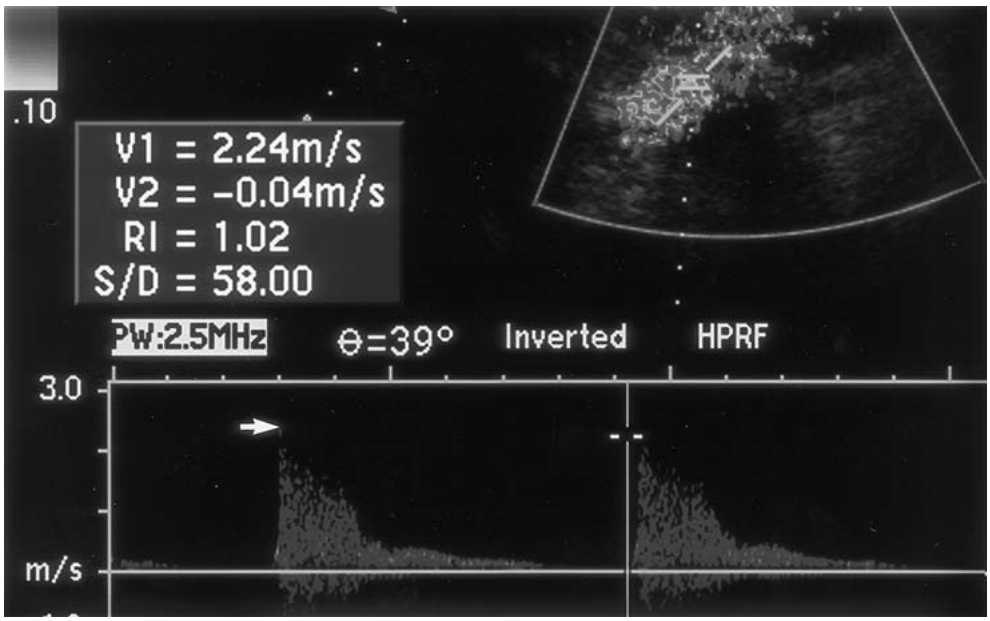

Fig. 15. Renal artery stenosis. Spectral Doppler US tracing of the renal artery anastomosis demonstrates increased velocity (*arrow*) at the site of anastomotic stenosis.

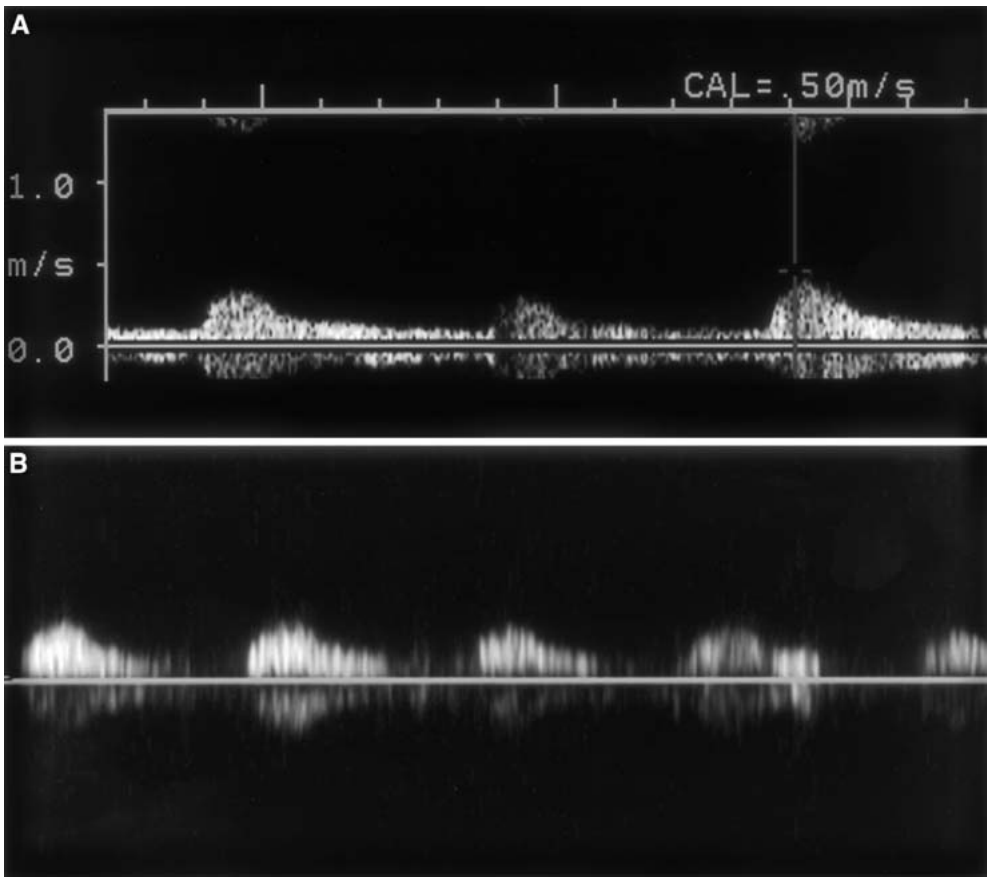

Fig. 16. Renal artery stenosis. **A, B** Spectral Doppler US tracing from an intrarenal artery shows spectral broadening and diminished amplitude of systole (tardus-parvus pattern) secondary to a proximal arterial stenosis.

nosis of vascular pathology at the expense of a more timely examination, and this may assume a more prominent role in the future [24, 30].

Gadolinium-enhanced 3D MRA can accurately assess arterial and venous components of the renal transplant graft [12]. MRA has been shown to compare favorably with DSA, the gold standard, in the evaluation of native renal artery and transplant renal artery stenoses and can also detect venous complications and perfusion defects [6, 10, 31, 32]. MRA can demonstrate the transplant artery in

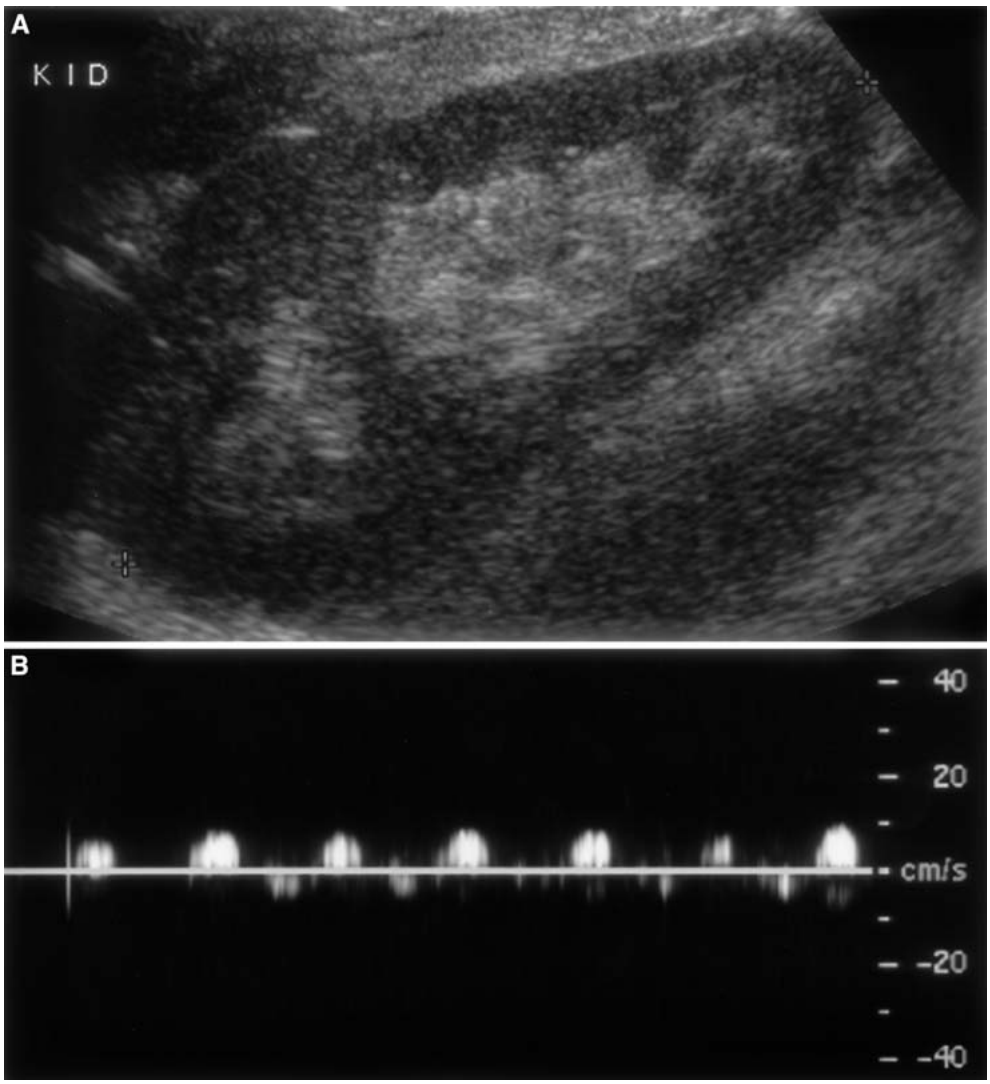

Fig. 17. Renal artery thrombosis. **A** Longitudinal gray-scale US shows normal size and echogenicity of the graft. **B** Spectral Doppler US tracing from an intrarenal artery is markedly abnormal with no normal discernible arterial flow.

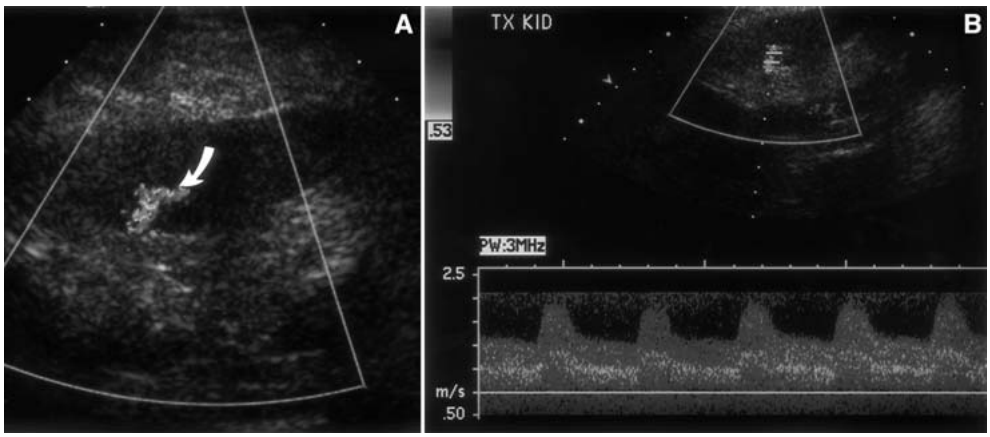

Fig. 18. AV fistula. **A** Color Doppler US shows a focus of disorganized color flow outside the borders of the normal renal vasculature (*arrow*). **B** Spectural Doppler US tracing over the fistula site displays characteristic arterial and venous components.

addition to the iliac arteries and lower abdominal aorta in a 20- to 30-s acquisition that can be performed during breath holding (Fig. 19). Gadolinium has been shown to be safe even in high doses in patients with renal failure [7]. Workstation postprocessing of the MRA data provides a summated depiction of the entire volume dataset, which can be displayed in cine fashion in any projection to best delineate vessel relations, separate overlying vessels, and depict tortuous vessels. Some investigators have advocated coronal oblique plane to ensure visualization of the

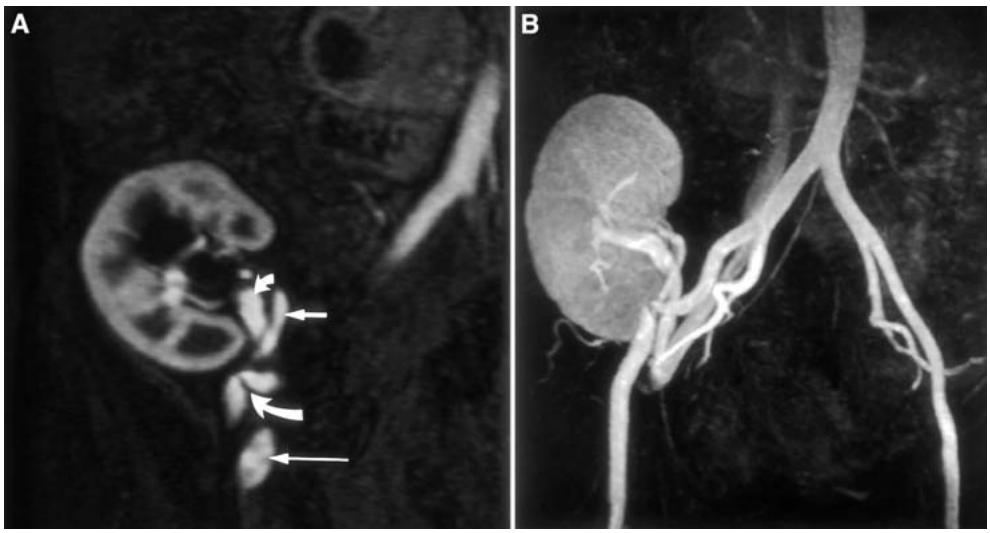

Fig. 19. External iliac artery stenosis. **A** Arterial phase MRA source image demonstrates kink and stenosis in the external iliac artery (*large curved arrow*). Note normal renal artery (*straight arrow*), renal vein (*small curved arrow*), and external iliac vein (*long arrow*). **B** Anteroposterior MIP further depicts the abnormality and relation of surrounding vessels.

Fig. 20. Renal artery stenosis. (**A**) Anteroposterior and (**B**) oblique MIP images show high-grade stenosis of the proximal renal artery (*straight arrow*). Flow is identified in distal artery (*curved arrow*).

anastomoses of interest [12]. Stenosis may appear as a focal narrowing or an abrupt cutoff at the anastomotic site with nonvisualization of the distal artery, depending on the amount of contrast flowing into the artery through the stenosis (Fig. 20). Alternatively, poststenotic dilatation may be seen. MRA has been shown to be more sensitive than US in the detection of native RAS [8]. MRA has also been shown to demonstrate perfusion in areas where Doppler US could not [24]. US has an overall sensitivity of 87% to 94% and a specificity of 86% to 100% in diagnosis of graft RAS compared with an MRA sensitivity and specificity of 67% to 100% and 75% to 100%, respectively [13, 23]. However the functional consequences of a stenosis, including asymmetry of size, enhancement, excretion, and loss of corticomedullary differentiation, can be assessed on MRA datasets and this is often the information clinicians are interested in to see if a patient will benefit from revascularization. This also enables the significance of borderline RAS to be evaluated. Other investigators have used two-dimensional cine phase-contrast sequences to assess renal artery flow, leading to decreased interobserver variability on stenosis grading [8].

Thromboses, which occur in up to 6% of cases, and their functional consequences are also well assessed by MRA, where characteristic findings can be seen [13, 28]. RAT manifests as a global lack of perfusion and the renal artery is not identified. Segmental or complete allograft infarction manifest as absent parenchymal and venous enhancement (Fig. 21). RVT typically causes enlargement of the graft with a delayed and persistent nephrogram. Frequently thrombus can be identified within the renal vein. False aneurysms and AV fistulae are also well visualized and demonstrate enlargement or shunting on

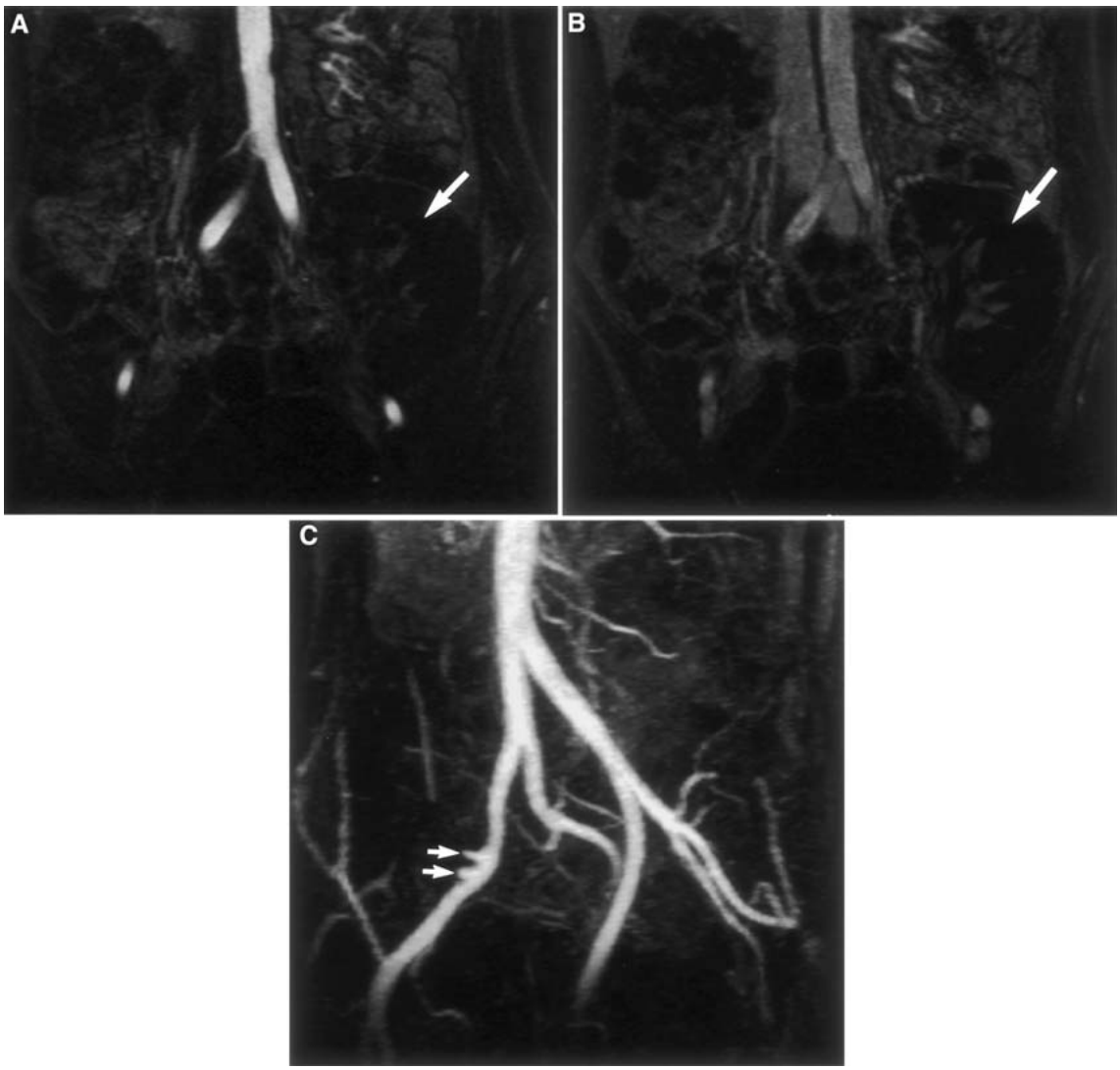

Fig. 21. Renal artery thrombosis. MRA in (**A**) arterial and (**B**) venous phases of enhancement visualize a complete lack of vascular flow to the graft (*arrow*). **C** Rotated MIP shows thrombosis to the proximal portion of two renal arteries (*arrows*).

MRA. MRA is, however, prone to certain pitfalls including poor bolus timing, overestimation of the degree of stenosis, and false positives due to susceptibility artifact from surgical clips adjacent to the anastomotic site [5, 6, 32]. Therefore when the arterial anastomosis appears stenotic, it is important to carefully evaluate the source MRA images to ensure that the abnormality in question is a true stenosis and not artifactual. Metallic clips can sometimes be seen to create a blooming artifact on T1-weighted images. Low arterial inflow due to end-organ resistance may also occasionally create false positives. Notwithstanding, we believe MRA accurately assesses transplant vascular anatomy without the potential risks of DSA and is less operator-dependent than US. However, DSA remains the gold standard for the diagnosis of transplant RAS and, like US, positive results on MRA need to be verified by DSA before surgical or percutaneous intervention [2, 9, 21, 23].

Parenchymal assessment

Parenchymal insults, including ATN, acute rejection, cyclosporin toxicity, or infection, are common in the postoperative period. Often the main differential lies between acute rejection and ATN. Because these entities require different therapeutic approaches, early and accurate diagnosis is essential. ATN occurs in the immediate transplant period as a result of ischemia before revascularization and is therefore seen more commonly in cadaveric transplants. Ten percent to 30% of transplant patients require dialysis in the early stages due to ATN [28]. It is generally self-limiting, with renal function recovering within days to weeks. Virtually every patient experiences some form of rejection, and differentiation from other causes of graft dysfunction continues to be a difficult clinical problem. Acute rejection is characterized by a relatively rapid rise in serum creati-

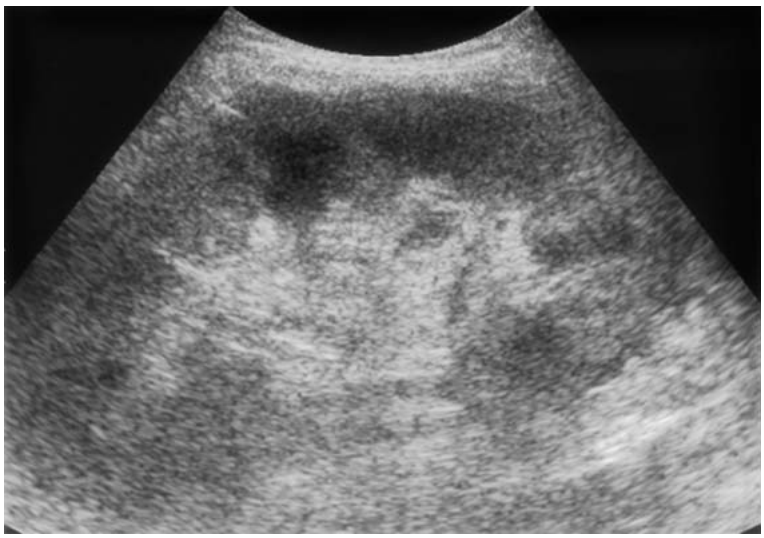

Fig. 22. Acute rejection. Longitudinal gray-scale US shows an enlarged graft with nonspecific changes in the corticomedullary region that was demonstrated by biopsy to represent acute rejection.

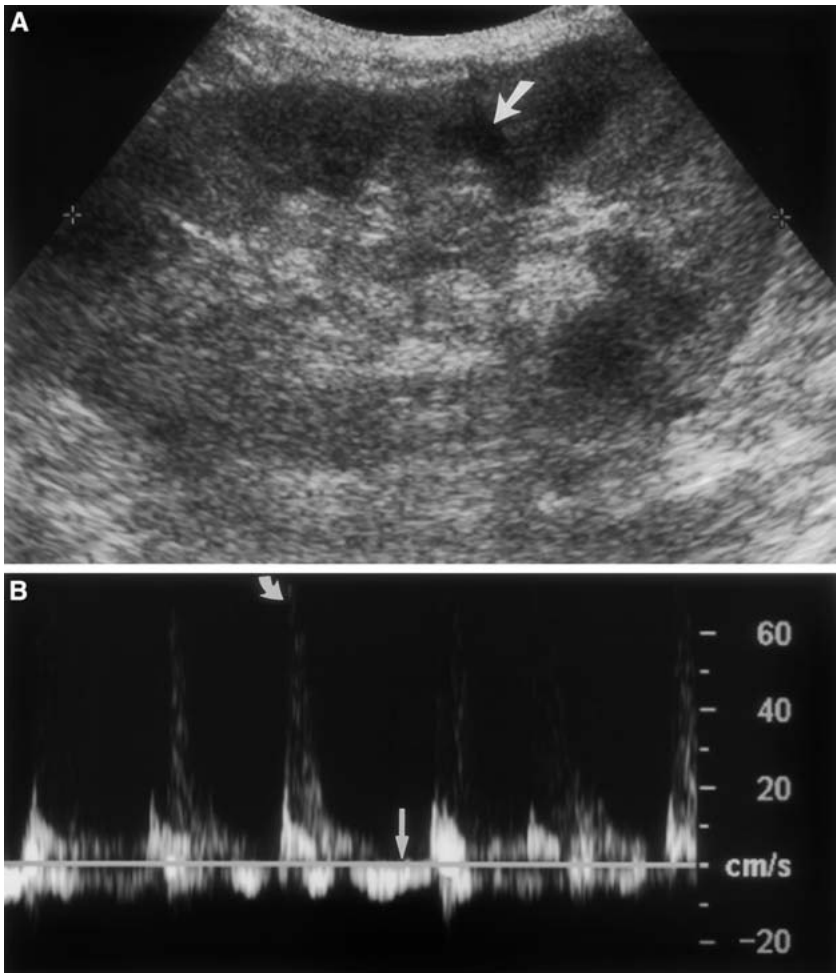

Fig. 23. Acute glomerular nephritis. **A** Longitudinal gray-scale US depicts an enlarged graft with loss of corticomedullary differentiation and abnormal echo-poor areas in the corticomedullary region (*arrow*). **B** Spectral Doppler US tracing shows a highly resistive waveform with increased PSV (*curved arrow*) and loss of end diastolic flow (*straight arrow*). These findings on US are nonspecific. The patient underwent graft biopsy, which showed acute glomerular nephritis.

nine (a rise ≥25% above baseline level occurring within 24 to 48 h). Acute rejection may affect up to 40% and peaks at 1 to 3 weeks after transplantation [1]. Chronic rejection relates to slow deterioration that progresses over months or years, eventually leading to azotemia and hypertension. Cyclosporine toxicity is caused by a reversible renovascular constriction acutely and an interstitial fibrosis chronically.

Although many US features of the parenchymal causes of dysfunction have been described, US cannot make the

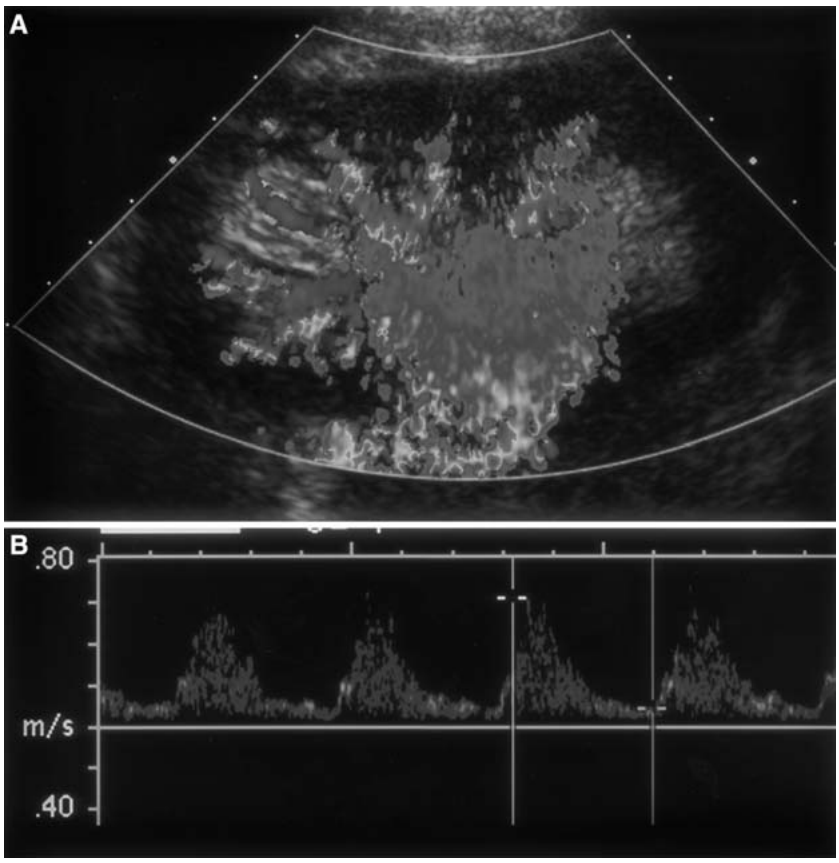

Fig. 24. **A** Longitudinal color Doppler US displays normal graft perfusion. **B** Spectral Doppler US tracing shows a nonspecific increase in RI. These findings persisted and subsequent biopsy showed ATN.

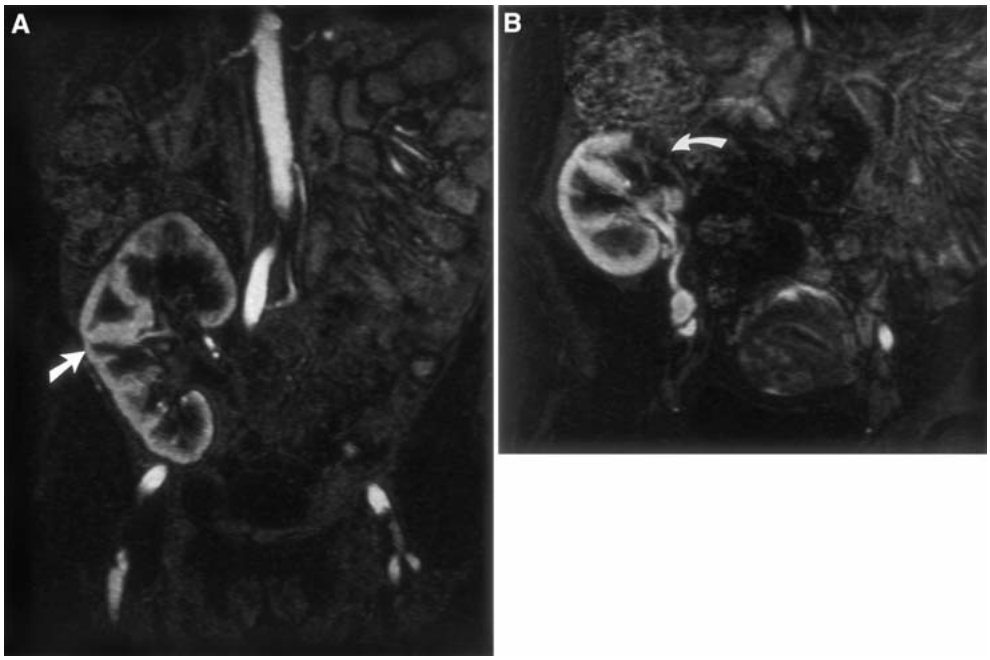

Fig. 25. **A** Coronal arterial phase MR renography shows diffuse graft cortical thinning (*arrow*). **B** Coronal arterial phase MR renography discloses upper pole scarring (*arrow*).

critical differentiation between ATN and acute rejection, which occur in the same time frame. Several studies have also failed to show any Doppler parameters that are useful in differentiating these entities [1]. The more severe and acute the rejection process, the more marked the US abnormalities. US characteristics of rejection include increased graft size, increased size and decreased echogenicity of the renal pyramids, decreased cortical echogenicity, and loss of corticomedullary differentiation [4] (Fig. 22). In general, these findings occur late, are

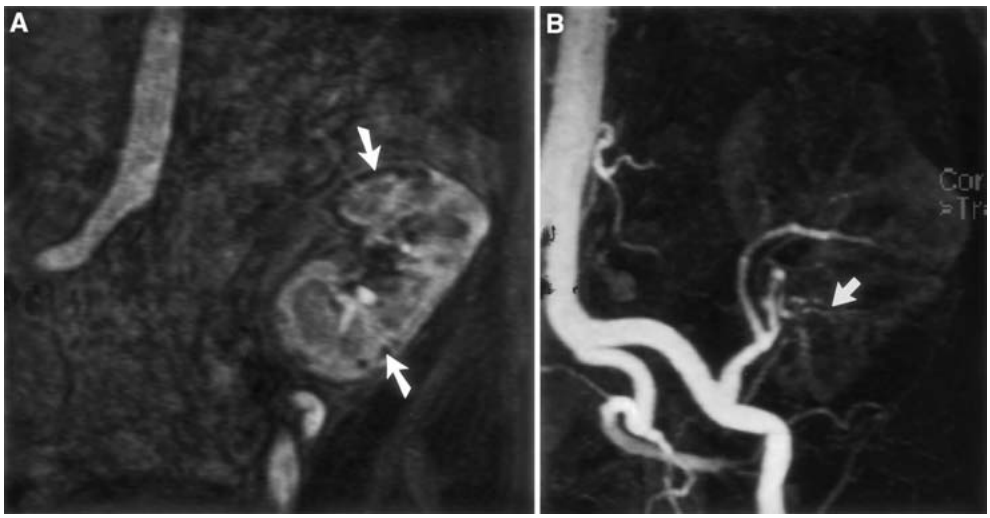

Fig. 26. Acute glomerular nephritis. **A** Coronal mixed phase MR renography shows decreased graft perfusion, abnormal corticomedullary differentiation, and diffuse areas of cortical hypoperfusion (*arrows*). **B** MIP displays a widely patent main renal artery with irregularity of the intrarenal arteries (*arrow*).

nonspecific, and may be caused by vascular or parenchymal dysfunction [28, 33] (Fig. 23). In severe rejection scattered heterogeneous areas of increased echogenicity may be seen in the cortex, reflecting areas of hemorrhage. With chronic rejection, there is a small kidney with cortical thinning, increased graft echogenicity, and a decrease in the number of intrarenal vessels. Cyclosporine toxicity may produce an enlarged kidney with increased cortical echogenicity and prominent medullary pyramids on US. Interval increases in RI, without a morphologic cause such as hydronephrosis, are indicative of graft dysfunction but may be caused by acute or chronic rejection, ATN, or cyclosporine toxicity [4, 14, 24, 28] (Fig. 24). Although US cannot differentiate the parenchymal causes of graft dysfunction, serial measurements of RI in conjunction with clinical and biochemical findings are useful, particularly in the early postoperative period, in monitoring and guiding the clinician as to whether or not a biopsy should be undertaken [28]. Biopsy is usually performed percutaneously under direct US guidance to ensure an adequate tissue sample is obtained and to minimize potential complications.

Postgadolinium T1-weighted coronal MR renography assesses renal parenchyma and parenchymal function by acquiring repeated images of the graft in arterial, venous, and mixed phases of contrast enhancement. This allows evaluation of renal size and contour and assessment of gadolinium uptake and excretion as a measure of renal function [34] (Fig. 25). The high spatial resolution of MRI allows visualization of gadolinium within distinct intrarenal regions, such as the cortex, medulla, and collecting system. MR renography therefore has the potential, unique among all noninvasive tests, to distinguish glomerular from tubulointerstitial pathology [20]. Renal length and width are measured and compared with previous dimensions, if available. On precontrast T1-weighted images, the cortex is of higher signal intensity than the medulla.

The normal renal cortex will enhance within 10 to 20 s after bolus injection followed by medullary enhancement at 20 to 30 s and collecting system opacification after 3 to 5 m. Deviations from this normal pattern of enhancement and excretion can therefore be assessed and studies have shown good correlation between signal intensity curves obtained with MR renography and 99mTc-DTPA renography [35]. Differences in parenchymal enhancement can indicate the severity of an arterial or ureteral stenosis. An abnormal nephrogram may be seen with ATN, rejection, or vascular insult [12] (Fig. 26). Focal abnormality of the nephrogram may occur secondary to infarct. On MRI, no renal enhancement or excretion of gadolinium in the presence of a widely patent renal artery implies likely rejection [6]. Loss of corticomedullary differentiation on MR renography, best assessed in the early cortical phase of enhancement, is said to be the most consistent sign of rejection and the degree corresponds to the severity of rejection [5, 36]. It has also been shown that MRI has a high accuracy in diagnosing rejection compared with US and scintigraphy, although overlap exists with ATN, nephritis, and cyclosporine toxicity [36]. Initial reports that rejection could be accurately diagnosed and differentiated from other parenchymal causes of graft dysfunction have not been substantiated by subsequent studies that found that loss of corticomedullary differentiation on MRI was a relatively nonspecific finding [8, 36, 37]. Delayed and decreased rate of medullary enhancement is also seen in dysfunctional kidneys, although this is also not specific to the exact etiology. Recently Szolar et al. [38] demonstrated distinct patterns of cortical and medullary enhancement to differentiate ATN from rejection, although differentiation was not possible when patients had both pathologies. Other investigators have successfully used similar parameters to differentiate rejection from cyclosporine toxicity, although the sample was small [39]. The technique of MR renography is still being

refined and uncertainties about technical issues such as signal intensity measurements, gadolinium dose optimization, and image analysis mean its exact clinical role has not yet been fully defined. Other MR renographic techniques are being developed to measure renal perfusion and glomerular filtration rate so that further functional data can be obtained [20]. Other investigators have used angiotensin-converting enzyme inhibitor MR renography to assess cortical signal intensity curves and determine the functional significance of RAS, with promising results [20]. It should also be noted that MRI has difficulty detecting parenchymal renal calculi/calcifications, although these are not commonly a cause of graft dysfunction.

This MR technique provides information about the functional significance of an arterial or ureteral stenosis that formerly required nuclear studies or EU. In contrast, US provides no real indication of renal function and only limited tissue characterization [15]. To date, no imaging or laboratory examination has been found that is sufficiently accurate in making the critical distinction between the parenchymal causes of graft dysfunction, and biopsy is still required [1, 4, 17, 33].

Conclusion

US maintains a critical role in graft evaluation, particularly in the immediate postoperative period when portable bedside studies can be easily performed, if required. US is also important in guiding percutaneous drainage and biopsy procedures. The advanced technical level of the various Doppler modes currently available, together with the more user-friendly equipment, will ensure that US remains an excellent technique for graft vascular assessment in the hands of an experienced operator.

A comprehensive MRI protocol, including 3D gadolinium-enhanced MRA, MRU, and MR renography, provides a rapid, noninvasive global assessment of the entire transplant including arterial and venous systems, parenchyma, collecting system, and peritransplant region as a single examination. Although MRI can detect parenchymal pathology and MR renography is promising in differentiating distinct parenchymal pathologies, biopsy may still be required for definitive diagnosis of rejection. We believe MRI offers a more complete and definitive evaluation of the graft than does US, with less reliance on additional investigations, particularly in collecting system and vascular assessments. We also believe combining these three components into a single examination offers improves patient convenience and has a potential cost saving. To some extent the choice of imaging modality will depend on local expertise and technology available. Both modalities avoid the use of ionizing radiation or iodinated contrast material and therefore preserve maximal renal function. US will probably remain the modality of choice in the immediate postoperative period, particularly in the unstable patient, with MRI reserved for cases in which US and clinical findings are discordant. In the follow-up period, for suspected and unsuspected complications, MRI may be more appropriate, particularly as techniques and functional assessment becomes more refined.

References

1. Baxter GM (2003) Imaging in renal transplantation. Ultrasound Q 19:123–138
2. Hohenwalter MD, Skowlund CJ, Erickson SJ, et al. (2001) Renal transplant evaluation with MR angiography and MR imaging. Radiographics 21:1505–1517
3. Schubert RA, Gockeritz S, Mentzel HJ, et al. (2000) Imaging in ureteral complications of renal transplantation: value of static fluid MR urography. Eur Radiol 10:1152–1157
4. Tublin ME, Dodd GD III (1995) Sonography of renal transplantation. Radiol Clin North Am 33:447–459
5. Neimatallah MA, Dong Q, Schoenberg SO, et al. (1999) Magnetic resonance imaging in renal transplantation. J Magn Reson Imaging 10:357–368
6. Dong Q, Schoenberg SO, Carlos RC, et al. (1999) Diagnosis of renal vascular disease with MR angiography. Radiographics 19:1535–1554
7. Prince MR, Narasimahar DL, Stanly JC, et al. (1995) Breath-hold gadolimum-enhanced MR angiography of the abdominal aorta and its major branches. Radiology 197:785–792
8. Zhang H, Prince MR (2004) Renal MR angiography. Magn Reson Imaging Clin North Am 12:487–503
9. Omary RA, Baden JG, Becker BN, et al. (2000) Impact of MR angiography on the diagnosis and management of renal transplant dysfunction. J Vasc Interv Radiol 11:991–996
10. Stafford Johnson DB, Lerner CA, Prince MR, et al. (1997) Gadolinium-enhanced magnetic resonance angiography of renal transplants. Magn Res Imaging 15:13–20
11. Hussain SM, Kock MC, Ijzermans JN, et al. (2003) MR imaging: a "one-stop shop" modality for preoperative evaluation of potential living kidney donors. Radiographics 23:505–520
12. Rusnack D, Israel GM (2004) Kidney transplantation: evaluation of donors and recipients. Magn Reson Imaging Clin North Am 12:505–514
13. Sandhu C, Patel U (2002) Renal transplantation dysfunction: the role of interventional radiology. Clin Radiol 57:772–783
14. McNamara MM, Lockhart ME, Robbin ML (2004) Emergency Doppler evaluation of the liver and kidneys. Radiol Clin North Am 42:397–415
15. Rothpearl A, Frager D, Subramanian A, et al. (1995) MR Urography: technique and application. Radiology 194:125–130
16. Gottlieb RH, Voci SL, Cholewinski SP, et al. (1999) Sonography: a useful tool to detect the mechanical causes of renal transplant dysfunction. J Clin Ultrasound 27:325–333
17. Letourneau JG, Day DL, Ascher NL, Castaneda-Zuniga WR (1988) Imaging of renal transplants. AJR 150:833–838
18. Hussain S, O'Malley M, Jara H, et al. (1997) MR urography. Magn Reson Imaging Clin North Am 5:95–106
19. Regan F, Bohlman ME, Khazan R, et al. (1996) MR urography using HASTE imaging in the assessment of ureteric obstruction. AJR 167:1115–1120
20. Huang AJ, Lee VS, Rusinek H (2003) MR imaging of renal function. Radiol Clin North Am 41:1001–1017
21. Patel NH, Jindal RM, Wilkin T, et al. (2001) Renal arterial stenosis renal allografts: retrospective study of predisposing factors and outcome after percutaneous transluminal angioplasty. Radiology 219:663–667
22. Patel U, Khaw KK, Hughes NC (2003) Doppler ultrasound for detection of renal transplant artery stenosis — threshold peak systolic velocity needs to be higher in low-risk or surveillance population. Clin Radiol 58:772–777
23. Low RN, Martinez AG, Steinberg SM, et al. (1998) Potential renal transplant donors: evaluation with gadolinium MR angiography and MR urography. Radiology 207:165–172

24. Jakobsen JA, Brabrand K, Egge TS, Hartmann A (2003) Doppler examination of the allografted kidney. Acta Radiol 44:3–12
25. Gottlieb RH, Lieberman JL, Pabico RC, Waldman DL (1995) Diagnosis of renal artery stenosis in transplanted kidneys: value of Doppler waveform analysis of the intrarenal arteries. AJR 65:1441–1446
26. de Morais RH, Muglia VF, Mamere AE, et al. (2005) Duplex Doppler sonography of transplant renal artery stenosis. J Clin Ultrasound 31:135–141
27. Loubeyre P, Abidi H, Cahen R, Tran Minh VA (1997) Transplanted renal artery: detection of stenosis with color Doppler US. Radiology 203:661–665
28. Baxter GM (2001) Ultrasound of renal transplantation. Clin Radiol 56:802–818
29. Orons PD, Zajko AB (1995) Angiography and interventional aspects of renal transplantation. Radiol Clin North Am 33:461–471
30. Correas J, Helenon O, Moreau JF (1999) Contrast-enhanced Ultrasonography of native and transplant kidney diseases. Eur Radiol 9(suppl 3):S394–S400
31. Chan YL, Leung CB, Yu SC, et al. (2001) Comparison of non-breath-hold high resolution gadolinium-enhanced MRA with digital subtraction angiography in the evaluation of allograft renal artery stenosis. Clin Radiol 56:127
32. Loubeyre P, Cahen R, Crozel F, et al. (1996) Transplant renal artery stenosis: evaluation of diagnosis with magnetic resonance angiography compared with color duplex sonography and arteriography. Transplantation 62:446–450
33. Huber A, Heuck A, Scheidler J, et al. (2001) Contrast-enhanced MR angiography in patients after kidney transplantation. Eur Radiol 11:2488–2495
34. Sharma RK, Gupta RK, Poptani H, et al. (1995) The magnetic resonance renogram in renal transplant evaluation using dynamic contrast-enhanced MR imaging. Transplantation 59:1405–1409
35. Heaf JG, Iversen J (2000) Uses and limitations of renal scintigraphy in renal transplantation monitoring. Eur J Nucl Med 27:871–879
36. Hricak H, Terrier F, Marotti M, et al. (1987) Posttransplant renal rejection: comparison of quantitative scintigraphy, US and MR imaging. Radiology 162:685–688
37. Rholl KS, Lee JKT, Ling D, et al. (1986) Acute renal rejection versus acute tubular necrosis in a canine model: MR evaluation. Radiology 160:113–117
38. Szolar DH, Preidler K, Ebner F, et al. (1997) Functional magnetic resonance imaging of human renal allografts during the post-transplant period: preliminary observations. Magn Reson Imaging 15:727–735
39. Agildere AM, Tarhan NC, Bozdagi G, et al. (1999) Correlation of quantitative dynamic magnetic resonance imaging findings with pathology results in renal transplants: a preliminary report. Transplant Proc 31:3312–3316